

Halogen-rich scapolite-biotite rocks from the Tongmugou Pb-Zn deposit, Qinling, north-western China: implications for the ore-forming processes

SHAO-YONG JIANG, M. R. PALMER

Department of Geology, University of Bristol, Bristol, BS8 1 RJ, U.K.

CHUN-JI XUE

Xi'an College of Geology, Xi'an, 710054, China

AND

YAN-HE LI

Institute of Mineral Deposits, Beijing, 100037, China

Abstract

Coexisting scapolite, biotite and hornblende in scapolite-biotite rocks from the Tongmugou Pb-Zn deposit, Qinling, northwestern China are characterized by high levels of chlorine. Scapolite composition varies from EqAn27 to EqAn47 with 47–80 wt.% Cl. The scapolite composition is a sensitive indicator of the NaCl activity in coexisting hydrothermal fluid. Biotite contains 0.3–1.2 wt.% Cl and also has high F contents (0.2–0.7 wt.%). The hornblende is a Cl-rich hastingsite with Cl > 3.5 wt.% and high (Na₂O + K₂O) contents (3.2–3.9 wt.%), high X_K [= K/(K + Na)] values (0.45–0.55) and high X_{Fe} [= Fe/(Fe + Mg)] values (0.76–0.79). The chlorine within these minerals is thought to be derived from evolved seawater. The scapolite-biotite rocks are products of Cl-rich alteration of volcanoclastic sedimentary rocks during submarine hydrothermal processes. Multiple-stage hydrothermal activity culminated with the circulation of a high-NaCl fluid that was also responsible for the formation of the massive sulphide deposits.

KEYWORDS: halogens, scapolite-biotite rock, hydrothermal fluids, China, Pb-Zn deposits

Introduction

THE Qinling Pb-Zn mineralization belt is one of the largest commercially exploited non-ferrous metal production areas in China. There are abundant scapolite-biotite rocks in close proximity to the orebodies in the eastern part of the belt, particularly around the Tongmugou deposit. A preliminary study showed that the scapolite in these rocks is Cl-rich (Xue *et al.*, 1989). It is well

known that Cl is strongly partitioned into aqueous fluids relative to solid phase (Munoz and Swenson, 1981; Volfinger *et al.*, 1985); therefore, minerals that concentrate Cl, such as scapolite, biotite and amphibole, may be particularly sensitive indicators of fluid composition and fluid-rock interaction (Sisson, 1987; Mora and Valley, 1989). We have used the chemistry of Cl-rich minerals from the scapolite-biotite rocks at Qinling to infer the origin of the rock and

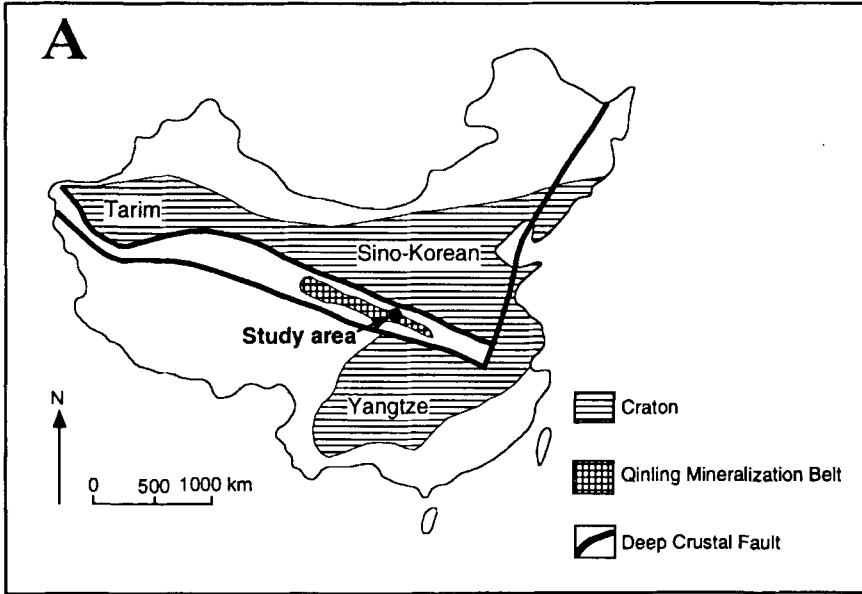


FIG. 1A. Geographic and geologic setting of the Qinling Pb-Zn mineralization belt in China.

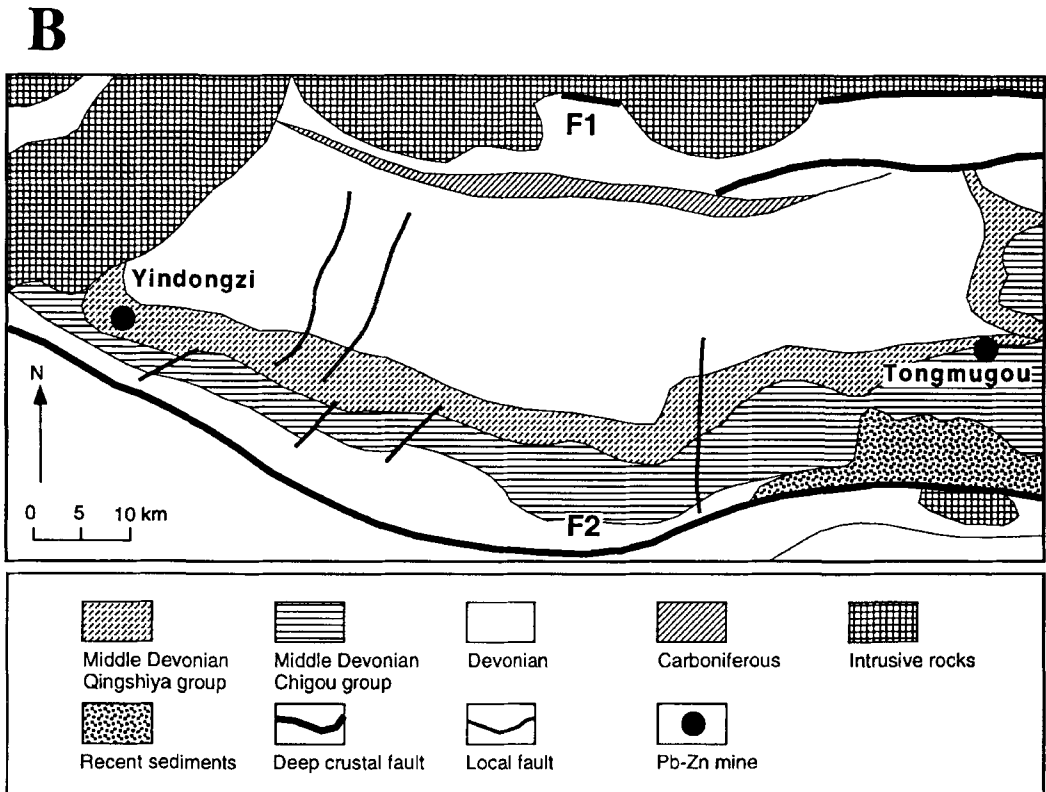


FIG. 1B. Geological map of the eastern part of the Qinling Pb-Zn mineralization belt.

constrain the nature of the hydrothermal fluids that led to the high Cl-levels in these minerals and also formed the associated Pb-Zn deposits.

Geologic setting

The Qinling Pb-Zn mineralization belt developed along a series of E-W trending Devonian rift basins ~500 km long. In the eastern part of this belt, two important deposits, the Yindongzi Pb-Zn-Ag ore deposit and the Tongmugou Zn-Pb ore deposit, occur within the Shunyang-Zhaishui rift basin (Fig. 1). In this basin a thick sedimentary column includes several volcanoclastic sedimentary horizons with tuffite interbeds, hydrothermal chemical sediments and sulphide ore beds. The main ore-bearing stratigraphic units belong to two middle-Devonian groups, known locally as the Chigou and Qingshiya Groups. The Chigou Group consists mainly of meta-argillitic siltstone, Ca-bearing meta-siltstone interbedded with ankerite-siltstone and limestone, and scapolite-biotite rock. The Qingshiya Group is composed of psammopelitic slate, siltstone interbedded with albite-bearing rock, siliceous rock and scapolite-biotite rock in the lower portion (Fig. 2) and silt-argillite, phyllite and siderite in the upper portion (not shown in Fig. 2). The sulphide ore bodies are located in the middle to lower portion of this latter group (Fig. 2), whereas some magnetite, baryte and siderite orebodies occur in the upper section (not shown in Figure 2). The scapolite-biotite rocks occur at several levels within the Chigou and Qingshiya Groups (Fig. 2); from their geochemical composition the protolith is thought to have been a volcanoclastic sedimentary rock (Xue *et al.*, 1989). The Devonian volcano-sedimentary sequence has undergone early diagenesis and later greenschist-facies metamorphism which have modified the host rocks and sulphide ores to varying degrees. The timing of metamorphism is poorly constrained, but is thought to be Hercynian (Zhang *et al.*, 1989).

Petrology of the scapolite-biotite rocks

Scapolite-biotite rocks are widespread in the eastern part of the Qinling Pb-Zn mineralization belt, especially around the Tongmugou deposit. They form stratiform bodies interbedded within mid-Devonian meta-siltstones and meta-argillites (Fig. 2). The mineral assemblage consists of scapolite and biotite, with varying amounts of quartz, calcite, hornblende and epidote. In the Tongmugou area scapolite is also commonly associated with pyrite and sphalerite. The relative amounts of the different minerals vary along strike

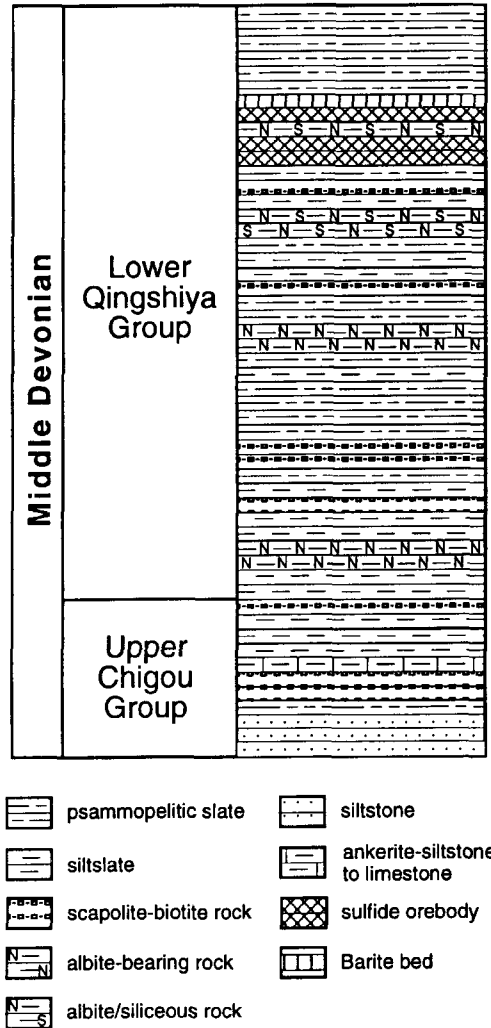


FIG. 2. Schematic stratigraphic column of the Qinling Tongmugou mid-Devonian rocks. (Note: thickness of some rock strata has been exaggerated for clarity).

and vertically. In general, two types of these rocks can be distinguished: scapolite-biotite rock and biotite rock containing little or no scapolite. The scapolite-biotite rock may be further divided into hornblende-bearing and hornblende-absent scapolite-biotite rock. Scapolite occurs as large, subhedral porphyroblasts within a finer matrix of biotite and minor quartz (Fig. 3). The porphyroblasts are up to 2.5 cm long, but are more typically <0.2 cm in diameter. The scapolite porphyroblasts show optical and chemical zonation with a darker coloured core (Fig. 3). Some scapolite crystals appear to be pseudomorphs after feldspar.

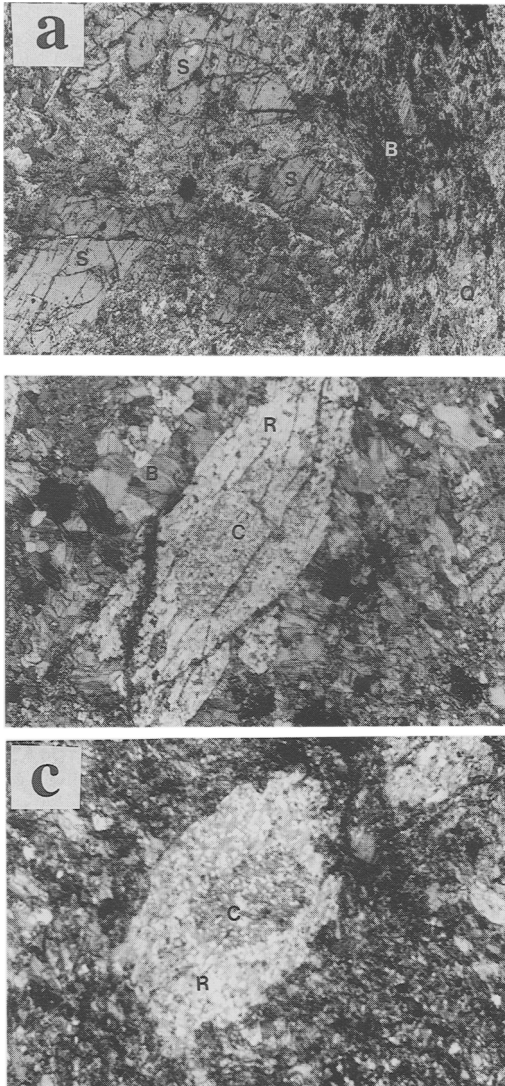


FIG. 3. (a) Large subhedral porphyroblasts of scapolite and finer matrix of biotite and quartz. Note the crosscutting biotite-quartz and carbonate vein within the scapolite. S—scapolite, B—biotite (field of view = 1.75 mm); (b) Zoned euhedral scapolite crystal in scapolite–biotite rock with a darker core and lighter rim. C—core of scapolite, R—rim of scapolite (field of view = 4.5 mm); (c) Zoned subhedral scapolite crystal in scapolite–biotite rock with a darker core and lighter rim. C—core of scapolite, R—rim of scapolite (field of view = 4.5 mm)

Geochemistry of the scapolite–biotite rocks

The scapolite–biotite rocks have high Na_2O (1.4–3.7 wt.%) and Cl (2.0–3.9 wt.%) contents compared with the local meta-argillite rocks ($\text{Na}_2\text{O} = 1.3$ wt.% and Cl = 0.06 wt.%) (Xue *et al.*, 1989). The chemical composition and REE pattern of the rocks indicate that the protolith was probably a volcanoclastic sediment. The REE pattern shows a positive Eu anomaly reflecting the former presence of volcanoclastic plagioclase, which was altered to scapolite during later hydrothermal activity (Xue *et al.*, 1989). In this study we report chemical compositions of minerals determined by a JEOL JXA-8600 electron microprobe (acceleration potential 15 kV, probe currents 20 nA, beam diameter 5 μm , counting times 15 s peak, 8 s background, and ZAF correction). Minerals and synthetic compounds SiO_2 (Si), MgAl_2O_4 (Al), SrTiO_3 (Ti), Fe_2O_3 (Fe), olivine (Mg), MnO (Mn), CaSiO_3 (Ca), albite (Na), adularia (K), MgF_2 (F) and a pantelerite glass (Cl) were used as standards. Microprobe analyses of biotite, scapolite and hornblende from the scapolite–biotite rock show that they are all Cl-rich minerals. Representative analyses are given in Table 1 and chemical variations are shown in Figs 4 to 9.

In Fig. 4 the equivalent anorthite content (EqAn = $100(\text{Al}-3)/3$) vs the mole fraction of CO_3 ($X_{\text{CO}_3} = 1-\text{Cl}$) in scapolite are plotted. The solid lines in

Fig. 4 indicate the stoichiometry of solid solutions (Evans *et al.*, 1969) between marialite (Mar) ($\text{Na}_4[\text{Al}_3\text{Si}_9\text{O}_{24}]\text{Cl}$) and meionite (Mei) ($\text{Ca}_4[\text{Al}_6\text{Si}_6\text{O}_{24}]\text{CO}_3$) and between marialite (Mar) and the intermediate component mizzonite (Miz). The Qinling scapolites are more Cl-rich than would be expected from the scapolite stoichiometry of Evans *et al.* (1969).

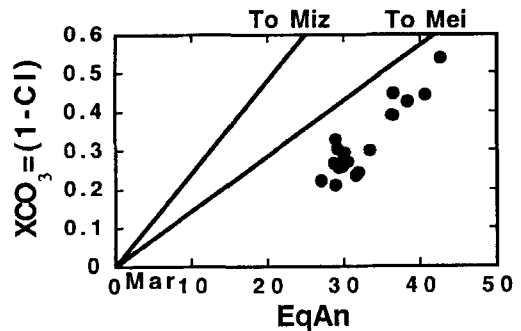


FIG. 4. EqAn = $100(\text{Al}-3)/3$ vs $X_{\text{CO}_3} = 1-\text{Cl}$ of scapolites from scapolite–biotite rocks, Tongmugou deposit, Qinling; note enrichment of Cl relative to the scapolite stoichiometry of Evans *et al.* (1969).

TABLE 1. Representative microprobe analyses of scapolite, biotite and hornblende

| Sample Number | Zn-3S1 core Scapolite | Zn-3S1 rim Scapolite | Zn-3S2 core Scapolite | Zn-3S2 rim Scapolite | Zn-37S1 core Scapolite | Zn-37S1 rim Scapolite | Zn-37S3 core Scapolite | Zn-37S3 rim Scapolite |
|---|-----------------------------|----------------------------|-----------------------------|----------------------------|------------------------------|-----------------------------|------------------------------|-----------------------------|
| SiO ₂ | 53.21 | 55.15 | 55.76 | 54.86 | 52.53 | 52.72 | 53.90 | 56.38 |
| Al ₂ O ₃ | 22.78 | 24.27 | 22.95 | 23.06 | 26.05 | 25.55 | 24.95 | 24.44 |
| FeO | 0.21 | 0.56 | 0.27 | 0.81 | 0.04 | 0.05 | 0.09 | 0.05 |
| MgO | 0.02 | 0.13 | — | 0.09 | 0.03 | — | 0.14 | 0.02 |
| MnO | — | 0.04 | — | — | — | — | — | — |
| CaO | 8.24 | 8.39 | 8.01 | 7.82 | 12.77 | 11.97 | 11.22 | 8.78 |
| Na ₂ O | 8.72 | 8.36 | 9.19 | 8.92 | 7.05 | 7.42 | 7.79 | 9.60 |
| K ₂ O | 0.43 | 0.45 | 0.57 | 0.63 | 0.43 | 0.53 | 0.47 | 0.50 |
| Cl | 2.95 | 2.95 | 3.25 | 3.04 | 1.95 | 2.35 | 2.34 | 3.29 |
| | 0.67 | 0.67 | 0.73 | 0.69 | 0.44 | 0.53 | 0.53 | 0.74 |
| Total | 95.89 | 99.630 | 99.270 | 98.540 | 100.410 | 100.060 | 100.390 | 102.310 |
| Structural formulae on the basis of 12(Si,Al) | | | | | | | | |
| Si | 7.976 | 7.902 | 8.081 | 8.024 | 7.574 | 7.638 | 7.764 | 7.941 |
| Al | 4.024 | 4.098 | 3.919 | 3.976 | 4.426 | 4.362 | 4.236 | 4.059 |
| Fe | 0.026 | 0.066 | 0.033 | 0.099 | 0.005 | 0.006 | 0.011 | 0.005 |
| Mg | 0.004 | 0.027 | — | 0.020 | 0.006 | — | 0.029 | 0.004 |
| Mn | — | 0.005 | — | — | — | — | — | — |
| Ca | 1.323 | 1.288 | 1.244 | 1.225 | 1.973 | 1.858 | 1.731 | 1.326 |
| Na | 2.533 | 2.323 | 2.583 | 2.530 | 1.970 | 2.084 | 2.177 | 2.621 |
| K | 0.081 | 0.083 | 0.105 | 0.118 | 0.080 | 0.098 | 0.087 | 0.090 |
| Cl | 0.750 | 0.716 | 0.799 | 0.755 | 0.477 | 0.576 | 0.572 | 0.786 |
| CO ₃ (a) | 0.250 | 0.284 | 0.201 | 0.245 | 0.523 | 0.424 | 0.427 | 0.214 |
| Me(b) | 34.11 | 36.55 | 32.21 | 33.67 | 49.18 | 46.07 | 43.89 | 33.00 |
| EqAn(c) | 34.13 | 36.60 | 30.63 | 32.53 | 47.53 | 45.40 | 41.20 | 35.30 |

(a) CO₃ = 1-Cl, (b) Me = 100(Ca + Mg + Fe + Mn)/(Na + K + Ca + Mg + Fe + Mn), (c) EqAn = 100(Al-3)/3

Few papers have reported Cl-rich biotite coexisting with Cl-scapolite. Ekstrom (1972) found Cl-contents of 0.3–0.5 wt.% in biotite coexisting with Cl-bearing scapolite in amphibolite-grade iron-formations in Sweden. Biotite from Qinling is more Cl-rich (0.3–1.2 wt.%; Table 1) than those reported by Ekstrom (1972) from Sweden. Unusually high-Cl biotite (0.18–5.5 wt.%) reported by Qen and Lustenhouwer (1992) from meta-exhalites in Sweden have very low F levels (<0.18 wt.%) whereas biotites from Qinling have F contents of 0.2–0.7 wt.%. Experiments show that F=OH and Cl=OH exchange in biotite is governed by several independent factors, including temperature, activities of the halogen acids, and the major element composition of the biotite (Munoz and Swenson, 1981; Munoz, 1984; Volfinger *et al.*, 1985). Fluorine is preferentially incorporated into biotites with high Mg/Fe ratios ('Fe-F avoidance'). The 'Mg-Cl avoidance' has been suggested from experimental studies although the compositional control of Cl in

biotite is not as well understood as that of F (Munoz and Swenson, 1981). Most biotite samples from Qinling have the predicted compositional trends of Fe-F and Mg-Cl avoidances (Fig 5).

Munoz (1984) defined IV(Cl) as a parameter for describing the relative Cl enrichment in biotite, corrected for the crystal-chemical Mg-Cl avoidance effect. This is manifest as a negative correlation between X_{Mg} and IV(Cl) values, where $IV(Cl) = -5.01 - 1.93X_{Mg} - \log(X_{Cl}/X_{OH})$ and $X_{Mg} = Mg/(Mg + \text{total Fe})$. The IV(Cl) was calculated from the biotite formula, taking $X_{Cl} = Cl/4$ and $X_{OH} = (4 - Cl - F)/4$. Lower IV(Cl) values indicate a greater Cl enrichment. Biotites from Qinling have 0.3 and 1.2 wt.% Cl and IV(Cl) values of -4.18 to -5.09, indicating high Cl enrichments, similar to biotites from meta-exhalites in Sweden, which have 0.14–5.5 wt.% Cl and IV(Cl) values of -3.35 to -5.40 (Oen and Lustenhouwer, 1992). In Qinling, strongly Cl-enriched biotites with IV(Cl) < -5.0 are also associated with Cl-rich hornblende and Cl-rich scapolite (e.g. sample Zn-3).

TABLE 1 (continued)

| Sample Number | Zn-3-B1 Biotite | Zn-3-B5 Biotite | Zn-37-B1 Biotite | Zn-37-B5 Biotite | Zn-3-H1 Hornblende | Zn-3-H2 Hornblende | Zn-3-H4 Hornblende | Zn-3-H6 Hornblende |
|--------------------------------|--------------------|--------------------|---------------------|---------------------|-----------------------|-----------------------|-----------------------|-----------------------|
| SiO ₂ | 36.52 | 37.79 | 36.37 | 37.54 | 43.74 | 34.20 | 34.79 | 35.53 |
| TiO ₂ | 1.18 | 1.26 | 1.01 | 1.45 | 0.30 | 0.30 | 0.43 | 0.41 |
| Al ₂ O ₃ | 15.93 | 15.34 | 17.10 | 17.28 | 12.66 | 13.94 | 14.05 | 14.16 |
| FeO | 17.80 | 15.61 | 15.45 | 15.89 | 22.33 | 23.05 | 24.43 | 25.34 |
| MgO | 11.44 | 13.46 | 16.12 | 14.93 | 3.57 | 4.11 | 3.77 | 3.74 |
| MnO | 0.09 | 0.06 | - | - | 0.17 | 0.08 | 0.08 | 0.14 |
| CaO | 0.30 | 0.09 | 0.08 | 0.07 | 9.85 | 9.73 | 10.60 | 10.95 |
| Na ₂ O | 0.11 | 0.13 | 0.12 | 0.13 | 1.22 | 1.25 | 1.33 | 1.43 |
| K ₂ O | 6.14 | 9.05 | 7.06 | 8.82 | 2.25 | 2.08 | 2.43 | 2.60 |
| F | 0.44 | 0.59 | 0.58 | 0.75 | - | - | 0.15 | - |
| Cl | 1.14 | 1.09 | 0.75 | 0.94 | 3.79 | 3.55 | 4.09 | 4.37 |
| | 0.44 | 0.49 | 0.41 | 0.53 | 0.86 | 0.80 | 0.99 | 0.99 |
| Total | 90.65 | 93.97 | 94.23 | 97.26 | 99.02 | 91.48 | 95.16 | 97.69 |

Structural formulae on the basis of 22 O for biotite and 23 O for hornblende

| | | | | | | | | |
|------------|--------|--------|--------|--------|-------|-------|-------|-------|
| Si | 5.698 | 5.710 | 5.419 | 5.464 | 6.670 | 5.830 | 5.753 | 5.752 |
| Al | 2.929 | 2.731 | 3.000 | 2.963 | 2.275 | 2.800 | 2.738 | 2.701 |
| Ti | 0.139 | 0.143 | 0.114 | 0.157 | 0.034 | 0.039 | 0.054 | 0.050 |
| Fe | 2.322 | 1.973 | 1.924 | 1.932 | 2.848 | 3.284 | 3.378 | 3.429 |
| Mg | 2.663 | 3.031 | 3.580 | 3.244 | 0.811 | 1.045 | 0.929 | 0.904 |
| Mn | 0.011 | 0.007 | - | - | 0.022 | 0.012 | 0.012 | 0.019 |
| Ca | 0.050 | 0.015 | 0.013 | 0.010 | 1.610 | 1.777 | 1.879 | 1.899 |
| Na | 0.032 | 0.036 | 0.036 | 0.037 | 0.361 | 0.414 | 0.426 | 0.449 |
| K | 1.222 | 1.745 | 1.342 | 1.637 | 0.436 | 0.451 | 0.512 | 0.537 |
| F | 0.219 | 0.280 | 0.271 | 0.344 | - | - | 0.078 | - |
| Cl | 0.302 | 0.280 | 0.189 | 0.232 | 0.980 | 1.024 | 1.147 | 1.198 |
| OH(a) | 3.479 | 3.440 | 3.540 | 3.424 | - | - | - | - |
| IV(CL) (b) | -4.980 | -5.090 | -4.990 | -5.050 | - | - | - | - |

(a) OH = 4-F-Cl, (b) IV(Cl) = $-5.01 - 1.93 * X_{Mg} - \log(X_{Cl}/X_{OH})$, $X_{Mg} = Mg/(Mg + \text{total Fe})$, $X_{Cl} = Cl/4$, $X_{OH} = OH/4$

Nijland *et al.* (1993) studied the halogen geochemistry of apatite, biotite, amphibolite and titanite. Their data show that the partitioning of Cl is described by the series apatite > amphibole > biotite > titanite. Leelanandam (1970) also suggested that Cl is preferentially partitioned into Ca-amphibole relative to biotite. Our data (Table 1) also show that Cl is slightly fractionated in favour of the coexisting hornblendes, although an opposite trend has also been reported in scapolite-biotite rocks from amphibolite-grade iron-formations in Sweden, where Cl is preferentially partitioned into biotite (Ekstrom, 1972).

Microprobe analyses reveal unusually high Cl contents of 3.5–4.4 wt.% Cl in the Qinling hornblendes, which are Cl-rich hastingsites according to the amphibole nomenclature of Leake (1978). The Cl-rich hastingsites also have high (Na + K) contents (0.76–0.97 atoms p. f. u.), high $X_K = K/(K + Na)$ values of 0.45–0.55, and

high $X_{Fe} = Fe/(Fe + Mg)$ values of 0.76–0.79. Chlorine-rich amphiboles are known from various rock types. A calcic amphibole from a skarn in Dashkesan has the highest Cl content (7.24 wt.%) so far recorded (Krutov, 1936); from the same skarn Cl-rich calcic amphibole with Cl-content of 5.34 wt.% was reported by Jacobson (1975). Dick and Robinson (1979) noted Cl-rich hastingsite in a sphalerite-bearing skarn in Southern Yukon. Chlorine-rich amphiboles in seafloor metamorphosed oceanic rocks have been reported from St. Paul's Rocks (a fracture zone exposure in the Atlantic Ocean) (Jacobson, 1975), rodingites and altered gabbros from the Atlantic at the Romanche Fracture Zone (Honnorez and Kirst, 1975), a DSDP gabbro from the Mid-Atlantic Ocean (Pritchard and Cann, 1982), gabbros from the Mid-Cayman Rise (Ito and Anderson, 1983), and metagabbros, amphibolites and metadiabase from the Mathematician Ridge (Vanko, 1986). In

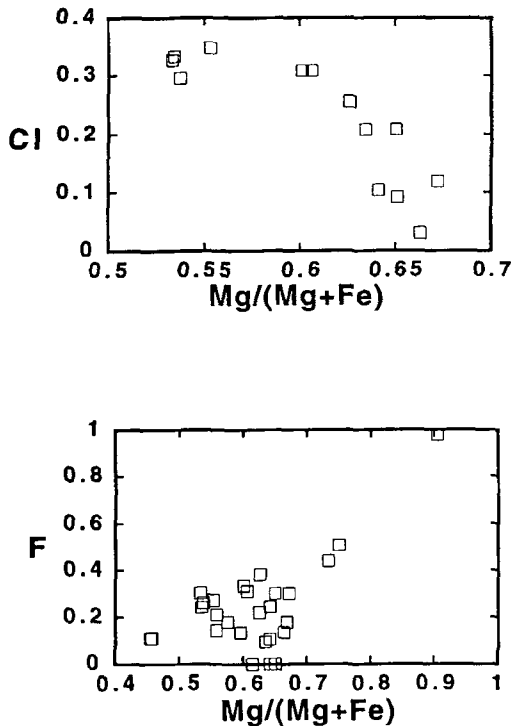


FIG. 5. Cl and F vs Mg/(Mg + Fe) diagram of biotite.

these cases Cl-rich amphiboles are thought to have formed by interaction of rocks with Cl-rich hydrothermal fluids. The geological setting of these rocks preclude an evaporite source for Cl so partially evolved seawater is the most probable source of Cl (Ito and Anderson, 1983; Vanko and Bishop, 1982).

There is a decrease of X_{Cl} with increasing X_{Mg} (Fig. 6), indicating that the Mg-Cl avoidance principle also applies to hornblende. Although the crystal-chemical control of the incorporation of Cl plays a role in the Cl content of amphibole

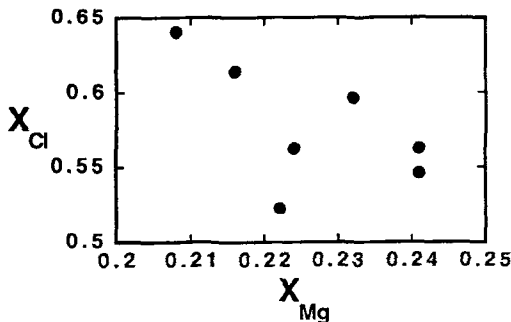


FIG. 6. X_{Cl} vs X_{Mg} diagram of hornblende. [$X_{Cl} = Cl/2$, $X_{Mg} = Mg/(Mg + total Fe)$].

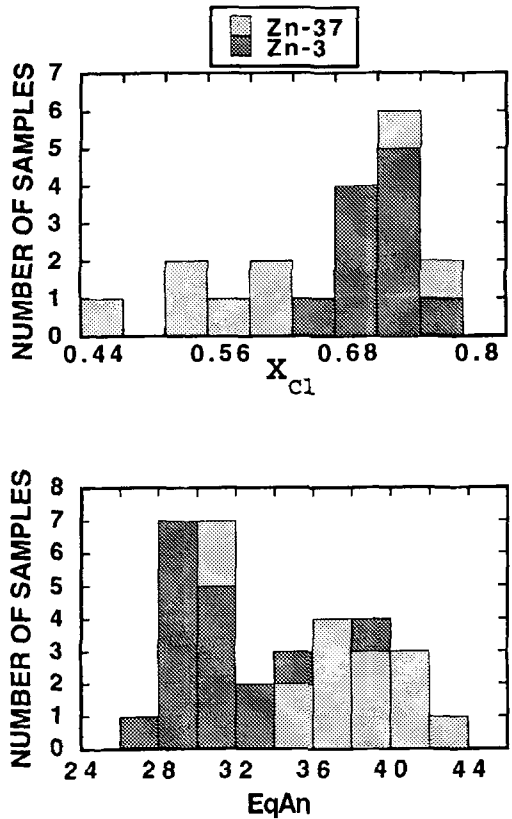


FIG. 7. Histograms of EqAn and X_{Cl} of scapolite.

(Volfinger *et al.*, 1985; Ito and Anderson, 1983), high Cl activity in hydrothermal fluid is also an important factor influencing the formation of Cl-rich hornblende (Vanko, 1986). The composition of co-existing scapolite and hornblende may reflect the NaCl activity of the hydrothermal fluids from which they crystallized. Figure 7 shows that the scapolite composition varies with the mineral assemblage. In sample Zn-3 the mineral assemblage is scapolite + biotite + hornblende + epidote, that in sample Zn-37 is scapolite + biotite with minor epidote, but no hornblende. Scapolites in Zn-3 are more NaCl-rich than those in Zn-37 (higher X_{Cl} and lower EqAn), suggesting that the NaCl activity was higher at the time of Cl-hornblende crystallization. The chemical zonation of scapolite also reveals changes of salinity of hydrothermal solution at different stages in the evolution of the deposit. In sample Zn-37 the relative difference between the core and rim is 2-6% EqAn and 0.1-0.2 X_{Cl} (Table 1). The core is more Ca-rich and the rim is more Cl-rich, indicating that the NaCl activity

became stronger during the crystallization of scapolite from core to rim. The chemical zonation in sample Zn-3 is not as apparent as in sample Zn-37. During the hydrothermal stage when the Cl-rich Ca-hornblende formed, a Cl-enriched environment may have formed by partial dissolution of the Cl-rich biotite.

Ito and Anderson (1983) suggested that Cl occupies the O₃ site in the amphibole chain and that incorporation of Cl into O₃ site may be structurally controlled and depend on the availability of Fe in the fluid phase. They inferred that Cl-rich amphiboles in submarine rocks formed under conditions where both Fe and Cl-rich solutions were available. We suggest that the Qinling Cl-rich hornblendes formed under similar conditions, i.e. during the stage of submarine hydrothermal activity when Fe-rich hydrothermal fluids were dominant in the system. A similar mechanism has been proposed for the origin of chemically-zoned tourmaline in the deposits (Jiang *et al.*, 1993).

Origin of the scapolite-biotite rocks

The occurrence of Cl-rich minerals in the scapolite-biotite rocks is an indication of high NaCl activity at the time of their crystallization. Several different models for the origin of high Na and Cl levels in similar rocks have been suggested. An evaporite origin has been proposed in some cases (Hietanen, 1967; Vanko and Bishop, 1982). The evidence to support this theory includes strict stratigraphic control on the occurrence of scapolite (Hietanen, 1967), salt casts and large skeletal halite crystals in stratigraphic equivalents (Grotzinger, 1986), hypersaline fluid inclusions (Roedder, 1984), the occurrence of abundant Mg- and Al-rich biotite (Moine *et al.*, 1981). Scapolite-biotite rock in the Tongmugou deposit of Qinling is restricted to certain sedimentary units, but there is no evidence for the prior existence of evaporites, such as salt casts and hypersaline fluid inclusions.

Tourmalines from the Qinling deposits have $\delta^{11}\text{B}$ values of between -7.6 and -8.8‰ (Jiang *et al.*, 1993), which is within the range reported for tourmalines from massive sulphide deposits associated within clastic metasedimentary rocks (Palmer and Slack, 1989) and do not support a marine evaporitic origin of the boron (Palmer, 1992). A non-marine evaporitic origin also seems improbable from the geological setting of the deposits and the occurrence of Cl-rich scapolite. Non-marine evaporitic sediments would be expected to give rise to CO₃-rich scapolite rather than Cl-rich scapolite since non-marine parageneses generally yield abundant sodium and calcium

carbonates rather than halides and sulphates (Vanko and Bishop, 1982). Another model for high NaCl activities is that their source might be provided by Cl-rich brines of either a magmatic or sedimentary origin. A magmatic origin is unlikely at Qinling as there are no igneous rocks within the mineralization areas. Hence, we propose a sedimentary origin for the high-salinity fluids.

The hydrothermal fluids may be derived from saline, Cl-rich, evolved seawater which passed through the footwall sediments in a submarine hydrothermal system, in a similar manner to hydrothermal fluids at present-day sediment-covered mid-ocean ridges. During the first stage of the hydrothermal activity, there was mixing between Mg-rich seawater and Fe-rich and Cl-rich hydrothermal fluids as indicated by the chemistry of zoned tourmaline in the deposits (Jiang *et al.*, 1993). This may have diluted the Cl concentration of the hydrothermal fluids to some extent. As hydrothermal activity progressed, Cl and Fe-rich hydrothermal fluids became more dominant (Jiang *et al.*, 1993) and the rock-fluid interactions were responsible for the formation of Cl-rich biotite and scapolite in the early stage and the crystallization of Cl-rich hornblende as well as more Cl-rich biotite and scapolite (as shown in sample Zn-3) from the late evolved fluids.

Conclusions

Scapolite-biotite rocks in the Qinling Pb-Zn deposits are the products of Cl rich alteration of volcanoclastic sedimentary rocks by saline submarine hydrothermal fluids. The high-Cl hydrothermal fluids may have efficiently transported large amounts of dissolved metals as chloride complexes (e.g. Chou and Eugster, 1977) and be responsible for the formation of the massive sulphide ores in Qinling. Hence, the evolution and distribution of this high-Cl hydrothermal system was important in determining the distribution and scale of ore-forming processes. The NaCl activity increased as the hydrothermal system evolved and the Cl-rich hornblendes formed as a result of elevated chlorine activity in the hydrothermal fluids. The formation of the high-grade sulphide ores in the Qinling deposits also took place during this stage. Thus, the hydrothermal rocks (including the massive sulphides) at Qinling were the result of multiple-stage submarine hydrothermal activity.

Acknowledgements

This work was supported by the China National Natural Science Foundation (grant no. 49103039),

the British Council and the Royal Society. We are also grateful to Steve Lane for his help with the microprobe analyses.

References

- Chou, I-Ming and Eugster, H. P. (1977) Solubility of magnetite in supercritical chloride solutions. *Amer. J. Sci.*, **277**, 1296–1314.
- Dick, L. A. and Robinson, G. W. (1979) Chlorine-bearing potassian hastingsite from a sphalerite skarn in Southern Yukon. *Canad. Mineral.*, **17**, 25–6.
- Ekstrom, T. K. (1972) The distribution of fluorine among some coexisting minerals. *Contrib. Mineral. Petrol.*, **34**, 192–200.
- Evans, B. W., Shaw, D. M. and Haughton, D. R. (1969) Scapolite stoichiometry. *Contrib. Mineral. Petrol.*, **24**, 293–305.
- Grotzinger, J. P. (1986) Shallowing-upward cycles of the Wallace Formation, Belt Supergroup, north-western Montana and northern Idaho. *Montana Bureau of Mines Geol. Spec. Pub.*, **94**, 143–60.
- Hietanen, A.H. (1967) Scapolite in the Belt Series in the St. Joe-Clearwater Region, Idaho. *Geol. Soc. Amer. Spec. Pap.*, **86**, 56pp.
- Honnorez, J. and Kirst, P. (1975) Petrology of rodingites from the equatorial Mid-Atlantic fracture zones and their geotectonic significance. *Contrib. Mineral. Petrol.*, **49**, 233–57.
- Ito, E. and Anderson, A. T. Jr. (1983) Submarine metamorphism of gabbros from the Mid-Cayman Rise: Petrographic and mineralogic constraints on hydrothermal processes at slow-spreading ridges. *Contrib. Mineral. Petrol.*, **82**, 371–88.
- Jacobson, S. S. (1975) Dashkesanite: High-chlorine amphibole from St. Paul's Rocks, Equatorial Atlantic, and Transcaucasia. *U.S.S.R. Mineral Science Investigations, Contrib. Earth Sci., Smithsonian Institute*, **14**, 17–20.
- Jiang, S-Y., Palmer, M. R., Li, Y-H. and Xue, C-J. (1993) Chemical compositions of tourmaline in the Yindongzi-Tongmugou Pb-Zn deposits, Qinling, China: Implications for the hydrothermal ore-forming processes. Submitted to *Mineral. Deposita*.
- Krutov, G. A. (1936) Dashkesanite: A new chlorine amphibole of the hastingsite group. *Mineral. Abstr.*, **6**, 438.
- Leake, B. E. (1978) Nomenclature of amphiboles. *Canad. Mineral.*, **16**, 501–20.
- Leelanandam, C. (1970) A chlorine rich biotite from Kondapalli, Andhra Pradesh, India. *Amer. Mineral.*, **55**, 1338–58.
- Moine, B., Sauvan, P. and Jarousse, J. (1981) Geochemistry of evaporite-bearing series: A tentative guide to the identification of metaevaporites. *Contrib. Mineral. Petrol.*, **76**, 401–12.
- Mora, C. I. and Valley, J. W. (1989) Halogen-rich scapolite and biotite: Implications for metamorphic fluid-rock interaction. *Amer. Mineral.*, **74**, 721–37.
- Munoz, J. L. (1984) F-OH and Cl-OH exchange in micas with applications to hydrothermal ore deposits. *Rev. Mineral.*, **13**, 469–93.
- Munoz, J. L. and Swenson, A. (1981) Chloride-hydroxyl exchange in biotite and estimation of relative HCl/HF activities in hydrothermal fluids. *Econ. Geol.*, **76**, 2212–21.
- Nijland, T. G., Jansen, J. B. H. and Majjer, C. (1993) Halogen geochemistry of fluid during amphibolite-granulite metamorphism as indicated by apatite and hydrous silicates in basic rocks from the Bamble Sector, south Norway. *Lithos*, **30**, 167–89.
- Oen, I. S. and Lustenhouwer, W. J. (1992) Cl-rich biotite, Cl-K hornblende, and Cl-rich scapolite in meta-exhalites, Nora, Bergslagen, Sweden. *Econ. Geol.*, **87**, 1638–48.
- Palmer, M. R. (1991) Boron isotope systematics of hydrothermal fluids and tourmalines: A synthesis. *Isotope Geosci.*, **14**, 111–21.
- Palmer, M. R., and Slack, J. F. (1989) Boron isotopic composition of tourmaline from massive sulfide deposits and tourmalinites. *Contrib. Mineral. Petrol.*, **103**, 434–51.
- Pritchard, H. M. and Cann, J. R. (1982) Petrology and mineralogy of dredged gabbro from Gettysburg Bank, eastern Atlantic. *Contrib. Mineral. Petrol.*, **79**, 46–55.
- Roedder, E. (1984) Low- to medium-grade metamorphic environments. *Rev. Mineral.*, **12**, 413–72.
- Sisson, V. B. (1987) Halogen geochemistry as an indicator of metamorphic fluid interaction with the Ponder pluton, Coast Plutonic Complex, British Columbia, Canada. *Contrib. Mineral. Petrol.*, **95**, 123–31.
- Vanko, D. A. (1986) High-chlorine amphiboles from oceanic rocks; products of highly-saline hydrothermal fluids? *Amer. Mineral.*, **71**, 51–59.
- Vanko, D. A. and Bishop, F. C. (1982) Occurrence and origin of marialitic scapolite in the Humboldt Lopolith, N.W. Nevada. *Contrib. Mineral. Petrol.*, **81**, 277–89.
- Volfinger, M., Robert, J-L., Velzeuf, D. and Neiva, A. M. R. (1985) Structural control of the chlorine content of OH-bearing silicates (micas and amphiboles). *Geochim. Cosmochim. Acta*, **49**, 37–48.
- Xue, C-J., Qi, S-J. and Liang, W-Y. (1989) A special scapolite-biotite rock in the mid-Devonian marine basin in eastern Qinling. *J. Xi'an Coll. Geol.*, **1**, 30–39.

Zhang, B-Y., Chen, D-X., Li, Z-J and Gu, X.

M.(1989) The regional geochemistry of the Zhashui-Shanyang mineralization belt. Chinese Geol. Univ. Pub. House, Beijing, 249pp. [*Manuscript received 4 January 1994: revised 28 March 1994*]